

Violation of Bell's inequality with a quantum dot in a tapered nanowire waveguide

Klaus D. Jöns,^{1,2,*} Lucas Schweickert,^{1,2,†} Marijn A. M. Versteegh,^{2,3,4} Dan Dalacu,⁵
Philip J. Poole,⁵ Angelo Gulinatti,⁶ Andrea Giudice,⁷ Val Zwiller,¹ and Michael E. Reimer^{2,8}

¹*Applied Physics Department, Royal Institute of Technology,
Albanova University Centre, Roslagstullsbacken 21, 106 91 Stockholm, Sweden*

²*Kavli Institute of Nanoscience, Delft University of Technology,
Lorentzweg 1, 2628CJ Delft, The Netherlands*

³*Quantum optics, Quantum Nanophysics and Quantum Information,
Faculty of Physics, University of Vienna,
Boltzmanngasse 5, 1090 Vienna, Austria*

⁴*Institute for Quantum Optics and Quantum Information,
Austrian Academy of Science, Boltzmanngasse 3, 1090 Vienna, Austria*

⁵*National Research Council of Canada, Ottawa, Canada, K1A 0R6*

⁶*Politecnico di Milano, Dipartimento di Elettronica Informazione e Bioingegneria,
piazza Leonardo da Vinci 32 - 20133 Milano, Italy*

⁷*Micro Photon Devices, via Stradivari 4 - 39100 Bolzano, Italy*

⁸*Institute for Quantum Computing and Department of Electrical & Computer Engineering,
University of Waterloo, Waterloo, N2L 3G1, Canada*

(Dated: June 14, 2022)

Abstract

We present a bright photonic nanostructure emitting polarization-entangled photon-pairs that violates Bell's inequality. An InAsP quantum dot generating the entangled photons is encapsulated in a tapered InP nanowire waveguide to ensure directional emission and efficient light extraction. The performed Bell test reveals a clear violation ($S_{\text{CHSH}} > 2$) of the Clauser-Horne-Shimony-Holt inequality by up to 9.3 standard deviations. Understanding the underlying recombination mechanism and exploring a novel quasi-resonant excitation at the wurtzite InP nanowire resonance, which reduces multi-photon emission, results in an entanglement fidelity of $F = 0.817 \pm 0.002$ without temporal post-selection. This allows for a violation of Bell's inequality by 25 standard deviations in the rectilinear-circular basis. Our results provide insight into the fundamental properties of nanowire quantum dots and highlight their possible application in measurement-device-independent quantum key distribution and quantum repeater protocols.

* Corresponding author: klausj@kth.se; This author contributed equally to this work.

† This author contributed equally to this work.

I. INTRODUCTION

Quantum light sources providing strongly entangled photons are essential components for quantum information processing [1, 2]. In particular, secure quantum communication schemes [3, 4] rely on light sources that meet stringent requirements. Quantum cryptography based on entangled photon-pair sources requires a violation of Bell’s inequality to guarantee secure data transfer [5]. Optically active semiconductor quantum dots satisfy several key requirements for these applications, namely: fast repetition rate up to 2 GHz [6], on-demand generation [7], electrical operation [8, 9], position control at the nano-scale [10], and entangled photon-pair emission [11, 12]. However, efficient photon extraction from these quantum dots requires additional photonic structures to be engineered around them, such as micro-cavities [13] or nanowire waveguides [14], to steer the light emission efficiently in the desired direction. Even though generation of entangled photons was already reported from such structures [15–17], a violation of Bell’s inequality in micro-cavity structures proved to be elusive due to multi-photon emission and cavity induced dephasing that resulted in a significant reduction of the source fidelity.

Here, we show that the emitted photon-pairs from a nanowire quantum dot violate Bell’s inequality without temporal post-selection. The violation is first verified by the stringent Clauser-Horne-Shimony-Holt (CHSH) measurement in the traditional basis [18]. Furthermore, we investigate the competing radiative decay processes involved in the entangled photon-pair generation that lead to increased entanglement fidelity without temporal post-selection. Utilizing quasi-resonant excitation of the quantum dot at the wurtzite InP nanowire resonance results in a reduced multi-photon emission and further enhances the fidelity of the entangled photon-pair emission. Our source enables us to collect two orders of magnitude more entangled photon-pairs than typically reported from standard quantum dot structures. In combination with the site-controlled growth in uniform arrays [19], the possibility to transfer the nanowire sources into devices accurately with a micro-manipulator, as well as the potential for electrical [20] and super-conducting contacting [21] of nanowires, our results on these nano-structured and bright entangled photon-pair sources highlight their great potential for future quantum emitter applications.

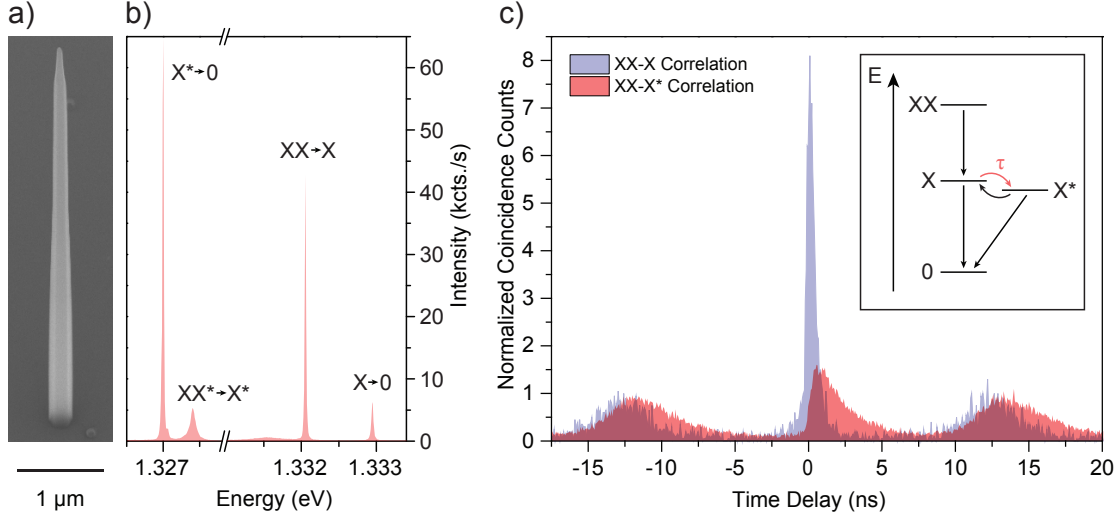


FIG. 1. a) SEM image of a pure wurtzite InP nanowire, containing a single InAsP quantum dot. The tapering of the nanowire shell allows for efficient light extraction. b) Quantum dot spectrum of the s-shell transitions. c) Cross-correlation measurements of biexciton (XX)–exciton (X) cascade (blue) and biexciton–charged exciton (X^*) cascade (red). The cross-correlation histograms are composed of 64 ps time bins. A fast exciton decay with $T = 0.41 \pm 0.08$ ns starts after the biexciton trigger. The observed delay of the charged exciton emission after the biexciton trigger is attributed to the charging time $\tau = 0.39 \pm 0.08$ ns of the quantum dot. The inset schematically shows the charging effect and the two possible competing recombination pathways.

II. PHOTONIC NANOSTRUCTURE

We study InAsP quantum dots embedded in pure wurtzite InP nanowires grown by selective-area chemical beam epitaxy. The (111)B InP substrate is masked with SiO_2 containing circular openings. Using a self-alignment process, a gold catalyst is centered in this circular opening allowing for precise positioning of the nanowire core and quantum dot [22]. Next, the growth conditions are modified to favor radial growth over axial growth resulting in a tapered, waveguiding shell around the nanowire core containing the InAsP quantum dot. Fig. 1 a) shows an SEM image of a tapered nanowire. In such photonic structures, the photons emitted by the quantum dot are guided by the high refractive index material of the nanowire and a small tapering angle towards the nanowire tip results in efficient light extraction [14]. In contrast to cavities, where achieving the necessary broadband frequency operation to realize bright entangled photon sources is extremely chal-

lenging, nanowire waveguides intrinsically provide this broadband frequency operation and have recently emerged as nanoscale sources with an excellent Gaussian far field emission profile [23, 24] for near-unity fiber coupling. For the investigated nanowire we found a light extraction efficiency of $18 \pm 3\%$ [16]. This efficiency can be further increased by adding a mirror below the nanowire [25, 26]. A detailed description of the full fabrication process can be found in Ref. 27.

Fig. 1 b) shows an s-shell emission spectrum of the investigated nanowire quantum dot. By performing cross-correlation measurements between the different transition lines, we found two competing recombination pathways in the quantum dot s-shell (illustrated in the inset of Fig. 1 c)): the biexciton (XX)–neutral exciton (X) cascade [28, 29] (blue curve in Fig. 1 a)), and the biexciton (XX)–charged exciton (X^*) cascade [30, 31] (red curve in Fig. 1 c)). Both measurements are taken under the same excitation conditions using the biexciton photon as the trigger at zero time delay. In the former case, the neutral exciton decays directly after the biexciton emission with a characteristic lifetime, T , of 0.41 ± 0.08 ns. In contrast, the charged exciton decay is delayed by the charging time, τ , of 0.39 ± 0.08 ns, which is the time it takes for the quantum dot to capture another charge carrier. This competing recombination pathway explains the short decay time observed for the neutral exciton. Since the observed charging time is much faster than the period of the exciton spin precession (≈ 3.5 ns) [16], induced by the small fine-structure splitting [32], the effect of the spin precession on the two-photon correlations is small. Moreover, the short exciton lifetime filters out additional cross-dephasing events. Therefore, our short exciton lifetime eliminates two of the main reasons for applying temporal post-selection to increase the degree of entanglement [17, 33].

III. COMPENSATION OF BIREFRINGENCE

Typically the entangled state obtained for conventional quantum dots is $(|HH\rangle + |VV\rangle)/\sqrt{2}$ [11, 12, 34, 35]. However, as previously reported [16], we observed a different entangled state from the quantum dot embedded in the waveguiding shell. This more general entangled state was described as $(|JJ\rangle + |WW\rangle)/\sqrt{2}$, where J and W are arbitrary orthogonal vectors in the Poincare sphere. This rotation of the conventional state might be introduced by birefringence of the nanowire waveguide arising from an asymmetric shape.

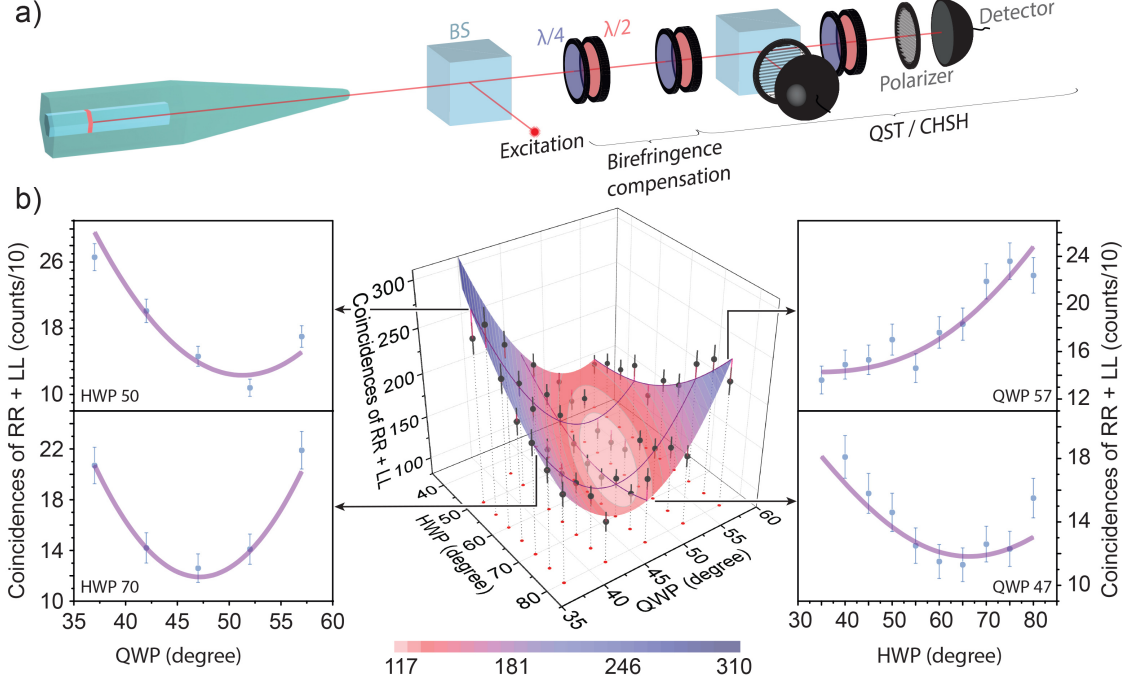


FIG. 2. a) Experimental setup for the Bell test and quantum state tomography (QST), including beam splitter (BS), half waveplates ($\lambda/2$), quarter waveplates ($\lambda/4$), polarizers and single-photon detectors. The first set of quarter and half waveplates is used to compensate the quantum state rotation introduced by the possible nanowire birefringence. b) 3D map showing the sum of coincidences at zero time delay for $|RR\rangle$ and $|LL\rangle$ correlations (black dots) as a function of quarter waveplate (QWP) and half waveplate (HWP) angles. Using a color-coded cosine surface fit we found the optimum waveplate configuration to compensate for the state rotation (minimum correlations in $|RR\rangle$ and $|LL\rangle$). Slices of the 3D map at constant HWP (QWP) angles are shown on the left (right) illustrating the good agreement between fit and data.

Using a set of waveplates we can compensate for this rotation and bring the entangled biexciton-exciton quantum state back to $(|HH\rangle + |VV\rangle)/\sqrt{2}$, allowing us to perform the CHSH measurements in the traditional basis [18].

In the following we optimize the waveplates to compensate for the observed state rotation. A schematic of the experimental setup is depicted in Fig. 2 a) where the emitted photons from the nanowire quantum dot are first sent through a $\lambda/4$ (QWP) and a $\lambda/2$ (HWP) waveplate before entering the analyzing polarization dependent cross-correlation setup (either for quantum state tomography (QST) or the Bell test (CHSH)). If the quantum state

of the photon pair is of the form $(|JJ\rangle + |WW\rangle)/\sqrt{2}$, with J and W being orthogonal polarization vectors, any state rotation can be compensated by minimizing the sum of the measured coincidences in $|RR\rangle$ and $|LL\rangle$ using these waveplates. Fig. 2 b) shows a three-dimensional (3D) map of these coincidences as a function of the QWP and HWP angles. The data is shown as black dots and the 3D cosine function fit of the data is color-coded. A clear minimum is observed in the light pink region, indicating the optimum waveplate angles required to compensate for the state rotation. The excellent result of the fit is emphasized in four cuts (dark purple) through the 3D map, displayed next to the map. The extracted QWP and HWP angles at the minimum of the surface fit will rotate the quantum state back to $(|HH\rangle + |VV\rangle)/\sqrt{2}$. This can be either verified by a full quantum state tomography or a simple fidelity approximation to the $(|HH\rangle + |VV\rangle)/\sqrt{2}$ state as shown in section VI.

IV. CHSH VIOLATION

After our successful compensation of the birefringence, we can perform the traditional four-parameter CHSH test, the standard test of local realism and device-independent secure quantum communication, to violate Bell's inequality.

The CHSH test requires 16 non-orthogonal cross-correlation measurements taken under the same experimental conditions. In the CHSH test the biexciton and exciton detection bases are independently rotated with respect to the rectilinear laboratory reference frame. The rotation angles α are given in real space angles in the schematic on the left of Fig. 3. The values 22.5° , 67.5° in red (0° , 45° in blue) correspond to the polarization angles added to the biexciton (exciton) polarization detection bases. To extract the degree of correlation C_b in all four possible combinations of these bases, we measure the coincidences of the biexciton (XX and \overline{XX}) and exciton (X and \overline{X}) photons. The degree of correlation C_b in one polarization basis b is extracted from the polarization dependent cross-correlation measurements (shown in Fig. 3):

$$C_b = \frac{g_{xx,x} + g_{\overline{x}\overline{x},\overline{x}} - g_{xx,\overline{x}} - g_{\overline{x}\overline{x},x}}{g_{xx,x} + g_{\overline{x}\overline{x},\overline{x}} + g_{xx,\overline{x}} + g_{\overline{x}\overline{x},x}},$$

where $g_{xx,x}$ and $g_{\overline{x}\overline{x},\overline{x}}$ ($g_{xx,\overline{x}}$ and $g_{\overline{x}\overline{x},x}$) are the coincidences of the co-polarized (cross-polarized) biexciton and exciton photons. Each measurement depicted in Fig. 3 was integrated for 7200s and the histograms are composed of 128 ps time bins. The insets magnify

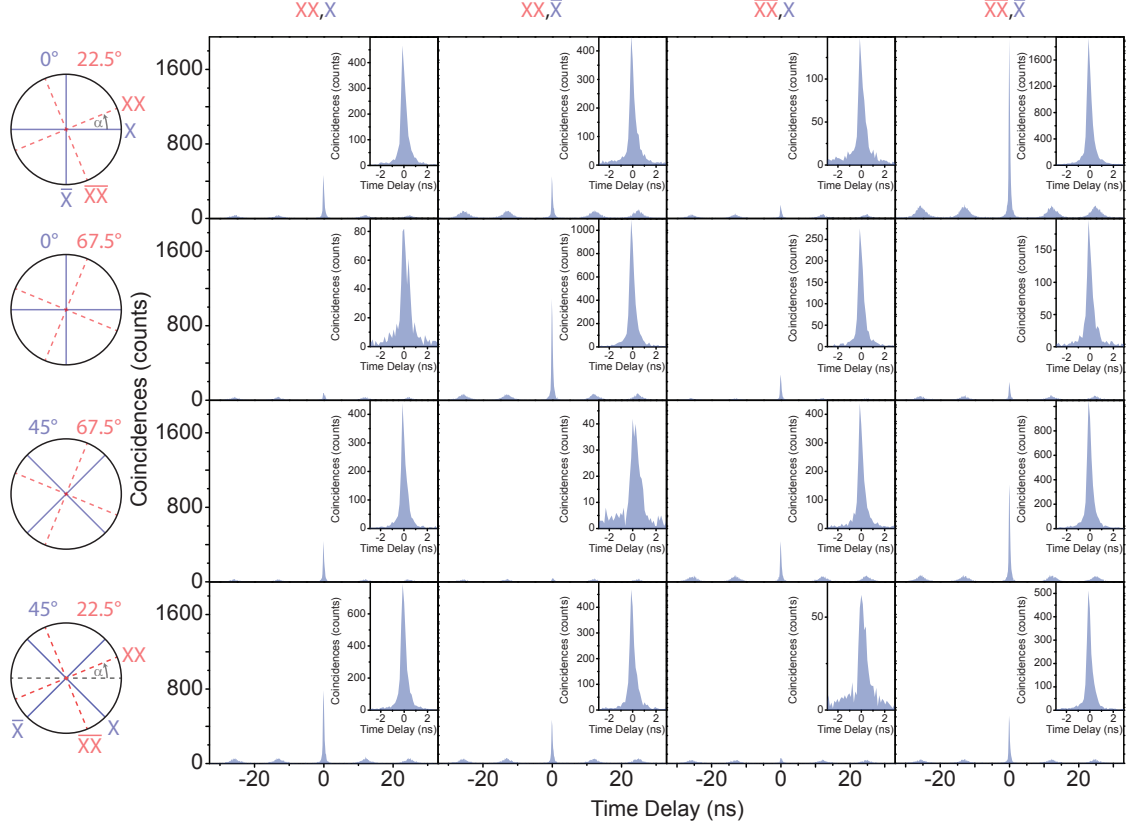


FIG. 3. The sixteen cross-correlation measurements needed for the violation of the Clauser-Horne-Shimony-Holt inequality. The angles on the left specify how much the polarization detection angle α for the exciton (blue) and biexciton (red) is rotated with respect to the rectilinear basis in the laboratory reference frame. For each set of rotation the degree of correlation C_b is extracted by measuring all four combinations between the biexciton (XX and \overline{XX}) and exciton (X and \overline{X}) photons. The insets show a magnification of the zero time delay peak.

the central peak at zero time delay. We calculate the Bell parameter with:

$$S_{\text{CHSH}} = C_{22.5^\circ, 0^\circ} - C_{67.5^\circ, 0^\circ} + C_{67.5^\circ, 45^\circ} + C_{22.5^\circ, 45^\circ} \leq 2.$$

In Table I we present the calculated Bell parameters extracted from the CHSH measurements in the linear plane of the Poincaré sphere for different time windows. Taking 100 % of the emitted photons into account, the calculated Bell parameter S_{CHSH} extracted from the CHSH measurements is 2.07 ± 0.02 . To violate the traditional CHSH inequality with the necessary certainty needed for applications in quantum key distribution we have to employ temporal post-selection. As shown in Table I we already achieve a sufficient violation by

TABLE I. Extracted Bell parameter from the CHSH measurements in the linear plane of the Poincaré sphere. The percentage of the correlation events taken into account for a certain time window is given in the second column.

Time window (ns)	Counts (%)	S_{CHSH}
4.48	100	2.07 ± 0.02
1.41	81	2.17 ± 0.02
0.38	38	2.28 ± 0.03
0.13	12	2.35 ± 0.06

8.5 standard deviations in a time window which is still 3.4 times longer than the excitonic lifetime, discarding only 19 % of the emitted photon-pairs. However, temporal post-selection complicates the implementation of quantum cryptography schemes severely. Therefore, we explore a quasi-resonant excitation scheme to significantly violate Bell’s inequality without the need for temporal post-selection.

V. QUASI-RESONANT EXCITATION

As seen in Table I temporal post-selection still increases the S_{CHSH} parameter even though the fine structure induced exciton dephasing at short time windows is negligible. Therefore, the false correlations in the CHSH measurements most likely originate from a re-excitation of the quantum dot and not from dephasing events.

Re-excitation can be reduced by minimizing the density of free charge carries in the nanowire, either by reducing the excitation power or by a more resonant excitation scheme. Fig. 4 a) shows the emission spectrum of the wurtzite InP nanowire resonances suitable for quasi-resonant excitation of the quantum dot. To verify our assumption that the false coincidences in the CHSH measurement originate from re-excitation of the quantum dot within one excitation laser pulse, we perform auto-correlation measurements on the biexciton. Fig. 4 b) depicts two of these measurements at different excitation laser wavelengths, while keeping the measured photon flux on the detectors constant. To maintain the same photon flux the laser power was reduced by 30 % for the quasi-resonant excitation. The top graph of Fig 4 b) shows the result for above-band excitation at a wavelength of 793 nm. The non-zero anti-bunching peak at zero time delay partly originates from re-excitation of

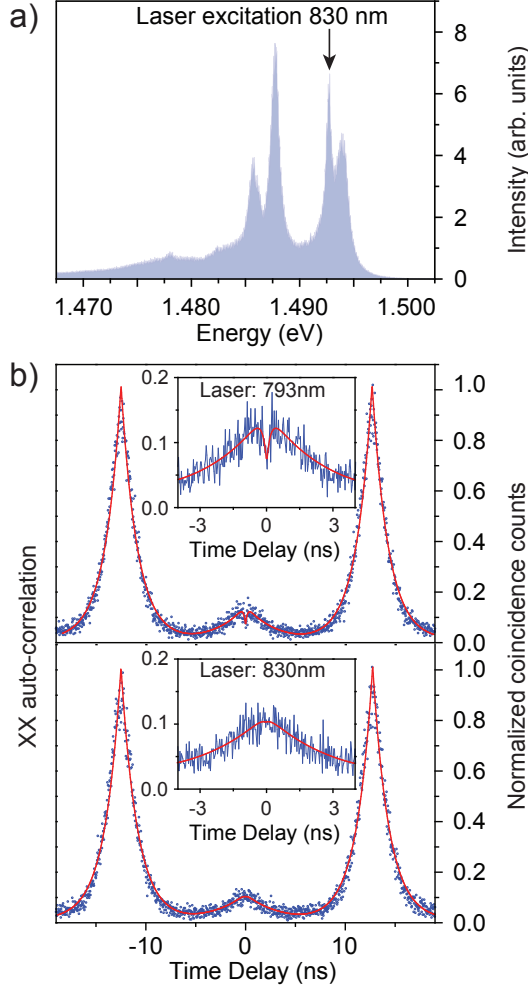


FIG. 4. a) Photoluminescence spectrum of the wurtzite InP nanowire resonances. The sharp resonance at 830 nm was addressed with a ps-pulse laser to excite the quantum dot quasi-resonantly. b) Auto-correlation histograms (time bins 32 ps) of the biexciton for above-band excitation at 793 nm (top) and quasi-resonant excitation in the InP nanowire wurtzite resonance at 830 nm (bottom). As shown in the insets the volcano-shaped dip at zero time delay, characteristic for re-excitation processes, is significantly reduced for the quasi-resonant excitation scheme in the lower panel.

the biexciton during the same laser excitation pulse. The signature of re-excitation is the volcano-shaped peak shown in the inset, leading to increased correlations near zero time delay. The dip in the zero time delay peak is caused by the biexciton needing time to decay before the re-excitation process. These additional biexciton photons start an additional cascade, which is independent of the first one, leading to false correlation counts in the CHSH

measurement and to a reduction of the measured degree of entanglement. Excitation of the wurtzite nanowire resonance at 830 nm (bottom graph of Fig 4 b)) significantly reduces the amount of re-excitation, indicated by the missing volcano-shape peak at zero time delay, as shown in the inset. The quasi-resonant excitation results in an overall improvement of the $g^{(2)}(0)$ by approximately 15 %. The remaining coincidences at zero time delay can be explained by background emission.

VI. IMPROVED BELL'S INEQUALITY VIOLATION

Using the quasi-resonant excitation scheme we characterize the improved entangled photon-pair emission of our photonic nanostructure. Fig. 5 shows the twelve non-normalized polarization dependent cross-correlation measurements [36] in three different bases (rectilinear, diagonal, and circular) needed for the fidelity approximation. The histograms are composed of 128 ps time bins and the first (second) letter denotes the biexciton (exciton) polarization. Strong positive correlations are visible in the rectilinear and diagonal basis and negative correlations in the circular basis, indicative of entanglement. From these measurements we calculate the fidelity, F , to the state $(|HH\rangle + |VV\rangle)/\sqrt{2}$ [37]:

$$F = (1 + C_{\text{rectilinear}} + C_{\text{diagonal}} - C_{\text{circular}})/4.$$

We find a fidelity of $F = 0.850 \pm 0.009$ to the state $(|HH\rangle + |VV\rangle)/\sqrt{2}$ for a time window of 0.13 ns. In Table II the fidelity to the state $(|HH\rangle + |VV\rangle)/\sqrt{2}$ for four different time windows, including the percentage of the correlation events taken into account, is given. For longer time windows the importance of our elegant quasi-resonant excitation of the nanowire is apparent. The fidelity is still as high as $F = 0.817 \pm 0.002$ for the full time window, a significant improvement as compared to above-band excitation, where $F = 0.762 \pm 0.002$. In addition to the reduced re-excitation induced coincidences, which occur at non-zero time delay, the quasi-resonant excitation should also reduce the amount of charge carriers surrounding the quantum dot. These reduced charge carriers in the environment potentially lead to fewer spin scattering and cross-dephasing events.

The remaining deviation from unity fidelity for the quasi-resonant case originates mostly from the multi-photon emission visible in the auto-correlation measurement (shown in Fig. 4 b)). We re-emphasize that the high degree of polarization-entangled photon-pairs

TABLE II. Calculated fidelity to $(|HH\rangle + |VV\rangle)/\sqrt{2}$ for four different time windows. The percentage of the correlation events taken into account for a certain time window is given in the second column. The calculated Bell parameters for all three basis combinations are always above the classical limit of 2.

Time window (ns)	Counts (%)	Fidelity to $(HH\rangle + VV\rangle)/\sqrt{2}$	S_{rc}	S_{dc}	S_{rd}
4.48	100	0.817 ± 0.002	2.25 ± 0.01	2.01 ± 0.01	2.16 ± 0.01
1.41	88	0.829 ± 0.002	2.26 ± 0.01	2.04 ± 0.01	2.21 ± 0.01
0.38	50	0.847 ± 0.003	2.36 ± 0.01	2.10 ± 0.02	2.30 ± 0.01
0.13	18	0.850 ± 0.005	2.37 ± 0.02	2.10 ± 0.03	2.32 ± 0.02

from our nanowire quantum dot, for the full time window, is benefited by the charging time τ . Controlling this effect could be achieved in future work with a gate to switch the photon emitting state population. The optimum gating time would depend on the excitonic fine-structure splitting. A similar gating technique was used to increase the visibility of two-photon interference [38].

Using the degree of correlation C_b extracted from the four corresponding cross-correlation measurements in that basis b , we can calculate the Bell parameters for our source. However, compared to the traditional CHSH measurement, no test of local hidden-variable theories is made, simply accepting the non-locality of quantum mechanics [39]. Following the work of Young and co-workers [40] three different Bell parameters: S_{RC} (rectilinear-circular), S_{DC} (diagonal-circular), and S_{RD} (rectilinear-diagonal), are given in Table II. Each one corresponds to a measurement in one of the three orthogonal planes of the Poincaré sphere. A value above 2 in these Bell parameters, as shown for all time windows for our entangled photon-pair source, confirms the non-classical character of the two-photon state. Employing this novel quasi-resonant excitation scheme we achieve a violation of Bells inequality in all three bases without temporal post-selection. In the rectilinear-circular basis violation by 25 standard deviations is achieved. In contrast to previous works that violate Bell's inequality with optically active self-assembled quantum dots [40–42], our nanowire quantum dot photon emission is slightly polarized. This effect has to be taken into account by performing four instead of two cross-correlation measurements to extract the degree of correlation in each basis, b . This more general approach to determine the Bell parameters is then not limited

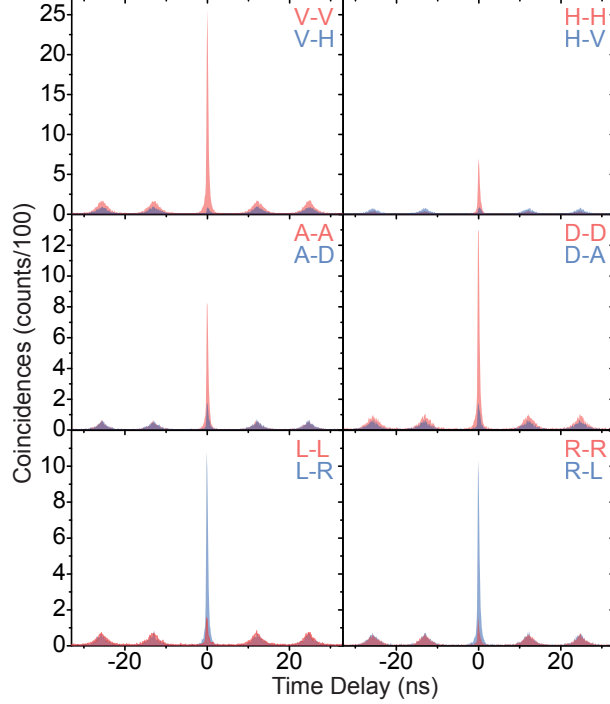


FIG. 5. Twelve cross-correlation measurements between the biexciton and exciton for different polarization detection bases, from top to bottom: rectilinear, diagonal and circular basis. The first (second) letter in the graphs stands for the polarization detection angle of the biexciton (exciton). The fidelity to the $(|HH\rangle + |VV\rangle)/\sqrt{2}$ state is $F = 0.817 \pm 0.002$ without temporal post-selection. These measurements are used to extract the Bell parameters in three orthogonal planes of the Poincaré sphere, given in Table II.

to unpolarized quantum light sources. We collect about 200000 entangled photon-pairs into the first objective. Due to this high brightness we want to highlight the capability of our nanowire quantum dot source as a referee source [43] for measurement device-independent cryptography. Assuming a setup consisting of four state-of-the-art detectors with quantum efficiency off 70%, a dichroic mirror for the confocal microscopy, and an efficient way to separate the biexciton and exciton our source will violate Bell's inequality in the rectilinear-circular basis by 5 standard deviation in less than 1 second. A violation by 5 standard deviation is currently seen as a significant test on the security of the communication channel. Our source can complete this task so fast due to the combination of the strong degree of entanglement and high photon-pair efficiency.

VII. CONCLUSION

We have demonstrated a bright entangled photon source in tapered nanowires capable of violating Bell's inequality by 25 standard deviations without the need for temporal post-selection. This is achieved by the quasi-resonant excitation in the wurtzite nanowire, which reduces re-excitation induced multi-photon emission, while maintaining the high entangled-photon pair flux. We compensated for the quantum state rotation possibly introduced by the nanowire birefringence, reconstructing the state $(|HH\rangle + |VV\rangle)/\sqrt{2}$ with a fidelity of $F = 0.817 \pm 0.002$ without temporal post-selection. Studying the correlations between different transitions revealed an intrinsic charging of the quantum dot on time scales shorter than the fine structure splitting induced excitonic spin precession time, explaining the high degree of entanglement observed. Our work highlights the applicability of novel nanowire quantum dots as bright entangled photon-pair sources suitable for measurement device-independent quantum cryptography and quantum information processing.

FUNDING INFORMATION

This research was supported by the Dutch Foundation for Fundamental Research on Matter (FOM projectruimte 12PR2994), Industry Canada, ERC, and the European Union Seventh Framework Programme 209 (FP7/2007-2013) under Grant Agreement No. 601126 210 (HANAS). K.D.J. acknowledges funding from the Marie Skłodowska Individual Fellowship under REA grant agreement No. 661416 (SiPhoN).

ACKNOWLEDGMENTS

The authors thank R. Trotta and A. W. Elshaari for scientific discussions.

AUTHOR CONTRIBUTIONS

M.A.M.V., K.D.J, V.Z. and M.E.R. conceived and designed the experiments. L.S., K.D.J, and M.E.R. performed the experiments. D.D. and P.J.P. fabricated the sample. K.D.J., M.E.R., and L.S. analyzed the data. A.Gu. and A.Gi. developed the detectors. M.E.R.

supervised the project. K.D.J., L.S., and M.E.R. wrote the manuscript with input from the other authors.

- [1] D. Bouwmeester, A. Ekert, and A. Zeilinger, *The physics of quantum information*, vol. 38 (Springer Berlin, 2000).
- [2] N. Gisin, G. Ribordy, W. Tittel, and H. Zbinden, “Quantum cryptography,” *Rev. Mod. Phys.* **74**, 145–195 (2002).
- [3] A. Acín, N. Brunner, N. Gisin, S. Massar, S. Pironio, and V. Scarani, “Device-independent security of quantum cryptography against collective attacks,” *Phys. Rev. Lett.* **98**, 230501 (2007).
- [4] V. Scarani, H. Bechmann-Pasquinucci, N. J. Cerf, M. Dušek, N. Lütkenhaus, and M. Peev, “The security of practical quantum key distribution,” *Rev. Mod. Phys.* **81**, 1301–1350 (2009).
- [5] A. K. Ekert, “Quantum cryptography based on bell’s theorem,” *Phys. Rev. Lett.* **67**, 661–663 (1991).
- [6] F. Hargart, C. A. Kessler, T. Schwarzbäck, E. Koroknay, S. Weidenfeld, M. Jetter, and P. Michler, “Electrically driven quantum dot single-photon source at 2 GHz excitation repetition rate with ultra-low emission time jitter,” *Appl. Phys. Lett.* **102**, 011126 (2013).
- [7] M. Müller, S. Bounouar, K. D. Jöns, M. Glässl, and P. Michler, “On-demand generation of indistinguishable polarization-entangled photon pairs,” *Nat Photon* **8**, 224–228 (2014).
- [8] Z. Yuan, B. E. Kardynal, R. M. Stevenson, A. J. Shields, C. J. Lobo, K. Cooper, N. S. Beattie, D. A. Ritchie, and M. Pepper, “Electrically driven single-photon source,” *Science* **295**, 102–105 (2002).
- [9] C. L. Salter, R. M. Stevenson, I. Farrer, C. A. Nicoll, D. A. Ritchie, and A. J. Shields, “An entangled-light-emitting diode,” *Nature* **465**, 594–597 (2010).
- [10] M. H. Baier, E. Pelucchi, E. Kapon, S. Varoutsis, M. Gallart, I. Robert-Philip, and I. Abram, “Single photon emission from site-controlled pyramidal quantum dots,” *Appl. Phys. Lett.* **84**, 648–650 (2004).
- [11] N. Akopian, N. H. Lindner, E. Poem, Y. Berlatzky, J. Avron, D. Gershoni, B. D. Gerardot, and P. M. Petroff, “Entangled photon pairs from semiconductor quantum dots,” *Phys. Rev. Lett.* **96**, 130501 (2006).

- [12] R. J. Young, R. M. Stevenson, P. Atkinson, K. Cooper, D. A. Ritchie, and A. J. Shields, “Improved fidelity of triggered entangled photons from single quantum dots,” *New Journal of Physics* **8**, 29 (2006).
- [13] E. Moreau, I. Robert, J. M. Grard, I. Abram, L. Manin, and V. Thierry-Mieg, “Single-mode solid-state single photon source based on isolated quantum dots in pillar microcavities,” *Applied Physics Letters* **79**, 2865–2867 (2001).
- [14] J. Claudon, J. Bleuse, N. S. Malik, M. Bazin, P. Jaffrennou, N. Gregersen, C. Sauvan, P. Lalanne, and J.-M. Gerard, “A highly efficient single-photon source based on a quantum dot in a photonic nanowire,” *Nat Photon* **4**, 174–177 (2010).
- [15] A. Dousse, J. Suffczynski, A. Beveratos, O. Krebs, A. Lemaitre, I. Sagnes, J. Bloch, P. Voisin, and P. Senellart, “Ultrabright source of entangled photon pairs,” *Nature* **466**, 217–220 (2010).
- [16] M. A. M. Versteegh, M. E. Reimer, K. D. Jöns, D. Dalacu, P. J. Poole, A. Gulinatti, A. Giudice, and V. Zwiller, “Observation of strongly entangled photon pairs from a nanowire quantum dot,” *Nat Commun* **5**, 5298 (2014).
- [17] T. Huber, A. Predojevic, M. Khoshnegar, D. Dalacu, P. J. Poole, H. Majedi, and G. Weihs, “Polarization entangled photons from quantum dots embedded in nanowires,” *Nano Letters* **14**, 7107–7114 (2014). PMID: 25395237.
- [18] J. F. Clauser, M. A. Horne, A. Shimony, and R. A. Holt, “Proposed experiment to test local hidden-variable theories,” *Phys. Rev. Lett.* **23**, 880–884 (1969).
- [19] M. T. Borgström, G. Immink, B. Ketelaars, R. Algra, and B. P.A.M., “Synergetic nanowire growth,” *Nat Nano* **2**, 541–544 (2007).
- [20] E. D. Minot, F. Kelkensberg, M. van Kouwen, J. A. van Dam, L. P. Kouwenhoven, V. Zwiller, M. T. Borgström, O. Wunnicke, M. A. Verheijen, and E. P. A. M. Bakkers, “Single quantum dot nanowire leds,” *Nano Letters* **7**, 367–371 (2007).
- [21] Y.-J. Doh, J. A. van Dam, A. L. Roest, E. P. A. M. Bakkers, L. P. Kouwenhoven, and S. De Franceschi, “Tunable supercurrent through semiconductor nanowires,” *Science* **309**, 272–275 (2005).
- [22] D. Dalacu, A. Kam, D. G. Austing, X. Wu, J. Lapointe, G. C. Aers, and P. J. Poole, “Selective-area vapourliquid-solid growth of in p nanowires,” *Nanotechnology* **20**, 395602 (2009).
- [23] M. Munsch, N. S. Malik, E. Dupuy, A. Delga, J. Bleuse, J.-M. Gérard, J. Claudon, N. Gregersen, and J. Mørk, “Erratum: Dielectric gaas antenna ensuring an efficient broad-

- band coupling between an InAs quantum dot and a Gaussian optical beam [Phys. Rev. Lett. **110**, 177402 (2013)],” Phys. Rev. Lett. **111**, 239902 (2013).
- [24] G. Bulgarini, M. E. Reimer, M. Bouwes Bavinck, K. D. Jöns, D. Dalacu, P. J. Poole, E. P. A. M. Bakkers, and V. Zwiller, “Nanowire waveguides launching single photons in a Gaussian mode for ideal fiber coupling,” Nano Letters **14**, 4102–4106 (2014).
- [25] J. Bleuse, J. Claudon, M. Creasey, N. S. Malik, J.-M. Gérard, I. Maksymov, J.-P. Hugonin, and P. Lalanne, “Inhibition, enhancement, and control of spontaneous emission in photonic nanowires,” Phys. Rev. Lett. **106**, 103601 (2011).
- [26] M. E. Reimer, G. Bulgarini, N. Akopian, M. Hocevar, M. B. Bavinck, M. A. Verheijen, E. P. Bakkers, L. P. Kouwenhoven, and V. Zwiller, “Bright single-photon sources in bottom-up tailored nanowires,” Nat Commun **3**, 737– (2012).
- [27] D. Dalacu, K. Mnaymneh, J. Lapointe, X. Wu, P. J. Poole, G. Bulgarini, V. Zwiller, and M. E. Reimer, “Ultraclean emission from InAsP quantum dots in defect-free wurtzite InP nanowires,” Nano Letters **12**, 5919–5923 (2012).
- [28] O. Benson, C. Santori, M. Pelton, and Y. Yamamoto, “Regulated and entangled photons from a single quantum dot,” Phys. Rev. Lett. **84**, 2513–2516 (2000).
- [29] E. Moreau, I. Robert, L. Manin, V. Thierry-Mieg, J. M. Gérard, and I. Abram, “Quantum cascade of photons in semiconductor quantum dots,” Phys. Rev. Lett. **87**, 183601 (2001).
- [30] M. Shirane, Y. Igarashi, Y. Ota, M. Nomura, N. Kumagai, S. Ohkouchi, A. Kirihaara, S. Ishida, S. Iwamoto, S. Yoroazu, and Y. Arakawa, “Charged and neutral biexcitonexciton cascade in a single quantum dot within a photonic bandgap,” Physica E: Low-dimensional Systems and Nanostructures **42**, 2563 – 2566 (2010). 14th International Conference on Modulated Semiconductor Structures.
- [31] E. Poem, Y. Kodriano, C. Tradonsky, B. D. Gerardot, P. M. Petroff, and D. Gershoni, “Radiative cascades from charged semiconductor quantum dots,” Phys. Rev. B **81**, 085306 (2010).
- [32] R. M. Stevenson, A. J. Hudson, A. J. Bennett, R. J. Young, C. A. Nicoll, D. A. Ritchie, and A. J. Shields, “Evolution of entanglement between distinguishable light states,” Phys. Rev. Lett. **101**, 170501 (2008).
- [33] M. Ward, M. Dean, R. Stevenson, A. Bennett, D. Ellis, K. Cooper, I. Farrer, C. Nicoll, D. Ritchie, and A. Shields, “Coherent dynamics of a telecom-wavelength entangled photon source,” Nat Commun **5**, 3316 (2014).

- [34] R. Hafenbrak, S. M. Ulrich, P. Michler, L. Wang, A. Rastelli, and O. G. Schmidt, “Triggered polarization-entangled photon pairs from a single quantum dot up to 30 K,” *New Journal of Physics* **9**, 315 (2007).
- [35] G. Juska, V. Dimastrodonato, L. O. Mereni, A. Gocalinska, and E. Pelucchi, “Towards quantum-dot arrays of entangled photon emitters,” *Nat Photon* **8**, 527–531 (2013).
- [36] A. Shields, R. Stevenson, and R. Young, “Entangled photon generation by quantum dots,” in “Single Semiconductor Quantum Dots,” , P. Michler, ed. (Springer Berlin Heidelberg, 2009), *NanoScience and Technology*, pp. 227–265.
- [37] A. J. Hudson, R. M. Stevenson, A. J. Bennett, R. J. Young, C. A. Nicoll, P. Atkinson, K. Cooper, D. A. Ritchie, and A. J. Shields, “Coherence of an entangled exciton-photon state,” *Phys. Rev. Lett.* **99**, 266802 (2007).
- [38] A. J. Bennett, R. B. Patel, A. J. Shields, K. Cooper, P. Atkinson, C. A. Nicoll, and D. A. Ritchie, “Indistinguishable photons from a diode,” *Applied Physics Letters* **92**, 193503 (2008).
- [39] H. Tanji, J. Simon, S. Ghosh, and V. Vuletić, “Simplified measurement of the Bell parameter within quantum mechanics,” *ArXiv e-prints* (2008).
- [40] R. J. Young, R. M. Stevenson, A. J. Hudson, C. A. Nicoll, D. A. Ritchie, and A. J. Shields, “Bell-inequality violation with a triggered photon-pair source,” *Phys. Rev. Lett.* **102**, 030406 (2009).
- [41] T. Kuroda, T. Mano, N. Ha, H. Nakajima, H. Kumano, B. Urbaszek, M. Jo, M. Abbarchi, Y. Sakuma, K. Sakoda, I. Suemune, X. Marie, and T. Amand, “Symmetric quantum dots as efficient sources of highly entangled photons: Violation of bell’s inequality without spectral and temporal filtering,” *Phys. Rev. B* **88**, 041306 (2013).
- [42] R. Trotta, J. S. Wildmann, E. Zallo, O. G. Schmidt, and A. Rastelli, “Highly entangled photons from hybrid piezoelectric-semiconductor quantum dot devices,” *Nano Letters* **14**, 3439–3444 (2014). PMID: 24845369.
- [43] M. Nawareg, S. Muhammad, E. Amselem, C. A. Nicoll, and M. Bourennane, “Experimental Measurement-Device-Independent Entanglement Detection,” *Sci Rep* **5**, 8048 (2015).